Mass Attraction Reduction by Integral Control in Spinning Drag-Free Satellites

J. DAVID POWELL*
Stanford University, Stanford, Calif.
AND
BENJAMIN O. LANGE†
Los Altos, Calif.
AND
PHILIP JHIN‡
U.S. Army, Redstone Arsenal, Ala.

In typical drag-free satellite designs, the largest internal force that perturbs the proof mass from a drag-free trajectory is the mass attraction of the satellite. Spinning the satellite with the spin vector normal to the orbital velocity vector eliminates most of the errors due to a constant body fixed gravitational force from the vehicle. If, however, there is a spatial gradient in the vehicle gravity field at the proof mass, spin does not necessarily eliminate this disturbance. An integral controller is discussed here which substantially attenuates the disturbances not eliminated by the spin. The mechanism by which mass attraction errors are reduced with integral control and the factors influencing its stability are examined. Mechanization errors of the integral controller show that drag-free performance with a disturbing acceleration level of 10^{-13} g (or position error of 1 km after one year) is quite feasible. In a nonspinning, nonintegral control drag-free satellite with mass attraction properties the same as that assumed here, drag-free performance of 10^{-10} g would result.

Nomenclature

c = $\cos(\omega_h t)$
c_2 = $\cos(2\omega_h t)$
C = $(\partial f_{ex}/\partial x + \partial f_{ey}/\partial y)/2$
ΔC = $(\partial f_{ex}/\partial x - \partial f_{ey}/\partial y)/2$
C_r = $(\partial f_{ex}/\partial y + \partial f_{ey}/\partial x)/2$
f_{bx}, f_{by} = body fixed disturbing specific forces on satellite
f_{cx}, f_{cy} = control specific force on satellite
f_{eh}, f_{ev} = horizontal and vertical components of force on proof mass due to mass attraction
f_{ei} = magnitude of inertially fixed force on proof mass
f_{ex}, f_{ey} = body fixed components of mass attraction on proof mass
$|f_i|$ = magnitude of f_{ix}, f_{iy}
f_{ix}, f_{iy} = inertially fixed disturbing specific forces on satellite
$\vec{F}_e$ = disturbing forces on proof mass
$\vec{F}_G$ = force of gravity on proof mass
h = in-track trajectory error
I_h, I_v = integral of f_{eh} and f_{ev}
I_{hc}, I_{vc} = integral of x_{bi} and y_{bi}
k_c = integral control gain
k_p = position gain
m_b = mass of proof mass
$\vec{r}$ = proof mass position with respect to an inertial reference
r_d = deadspace radius
s = $\sin(\omega_h t)$
s_2 = $\sin(2\omega_h t)$
W = $\begin{bmatrix} c & -s \\ s & c \end{bmatrix}$
x_b, y_b = position coordinates of proof mass in satellite fixed reference frame
x_{bi}, y_{bi} = proof mass position in an inertial reference frame
x_e, y_e = mass center location in satellite fixed reference frame
x_u, y_u = integral control bias coordinates
γ = velocity/position gain
η = complex expression for $x_b + jy_b$
ρ = constant describing proof mass position
ω_h = spin rate with respect to local horizontal
ω_o = orbital rate
ω_s = satellite angular velocity

Received January 31, 1972; revision received April 21, 1972.
Index category: Spacecraft Navigation, Guidance, and Flight-Path Control.

* Assistant Professor, Department of Aeronautics and Astronautics. Member AIAA.
† Independent Consultant.
‡ Aerospace Engineer, Missile Command.

Introduction

A DRAG-FREE satellite (DFS) contains an internal unsupported proof mass. The proof mass is under the sole influence of gravitational forces because it is shielded from external forces such as solar pressure and atmospheric drag by the outer satellite. A translation control system in the satellite senses the relative motion between the satellite and proof mass and actuates gas jets which force the satellite to follow the proof mass without touching it. Because the DFS follows a purely gravitational orbit, its orbit is substantially more predictable than conventional satellites. This feature provides the motivation for the current program at Stanford in cooperation with the Applied Physics Laboratory at Johns Hopkins University to design and build a drag-free satellite for navigation. Application of the technique for Geodesy investigations is also being studied. The drag-free performance requirements of this mission have motivated this research.

In current drag-free satellite designs, it is anticipated that the largest disturbing force on the proof mass will be due to the mass attraction of the satellite. This disturbance is body fixed and spinning the satellite averages the effect of any body fixed force in the plane of spin. The orbit in-track direction is significantly more sensitive to disturbing forces than other directions; therefore, spinning a drag-free satellite about an axis perpendicular to the in-track direction reduces the effect of mass attraction forces in the sensitive direction.[1] Systematic offsets of the proof mass required to actuate the gas jets during typical environmental forces such as atmospheric drag coupled with nonzero mass attraction force gradients produce disturbing forces on the proof mass which are not averaged by the spin. It is shown that, by relaxing the requirements on the mass attraction properties, an integral controller will reduce the precision required in locating and weighing the components of the satellite, a costly and time consuming task in the construction of the first drag-free satellite.

Equations of Motion

The relevant equations of motion of the drag-free satellite[2] are 1) the relative equations of the proof mass with respect to the satellite for control purposes, and 2) the equations of the proof mass alone for evaluating drag-free performance.

Relative Equations

The relative equations of motion of the proof mass with respect to the satellite are given assuming that the satellite mass center position is stationary and that $\dot{\omega}_s = 0$. The latter assumption implies that the satellite is spinning about a principal axis, stably oriented with respect to the orbit plane, and that disturbing torques are effectively cancelled by attitude control torques.[3] In this case, the equations of motion in the plane of spin expressed in a reference frame fixed to the satellite and centered at the proof mass position sensor null point, are

$$\ddot{x}_b - \omega_s{}^2 x_b - 2\omega_s \dot{y}_b = f_{ix} + f_{bx} + f_{cx} - \omega_s{}^2 x_e \quad (1a)$$

$$\ddot{y}_b - \omega_s{}^2 y_b + 2\omega_s \dot{x}_b = f_{iy} + f_{by} + f_{cy} - \omega_s{}^2 y \quad (1b)$$

The z-axis equation is uncoupled from the other axes and does not affect the items of interest in this paper; therefore, it will not be considered.

If a linear control law[4] (a weighted sum of position and velocity with respect to a nonrotating reference frame) is used, the control forces are

$$f_{cx} = -k_p[x_b + \gamma(\dot{x}_b - \omega_s y_b)] \quad (2a)$$

$$f_{cy} = -k_p[y_b + \gamma(\dot{y}_b + \omega_s x_b)] \quad (2b)$$

A constant external force with respect to a nonrotating reference frame causes sinusoidal forces f_{ix}, f_{iy}, as expressed in the rotating-body frame. With this type of disturbance, it can be shown by using Eqs. (1) and (2) that the steady-state error in x_b, y_b is

$$x_b = f_{ix}/k_p = [|f_i|/k_p]\cos(\omega_s t) = -f_{cx}/k_p \quad (3a)$$

$$y_b = f_{iy}/k_p = -[|f_i|/k_p]\sin(\omega_s t) = -f_{cy}/k_p \quad (3b)$$

Proof Mass Equations

The equation of motion of the proof mass is

$$m_b \ddot{\vec{r}} = \vec{F}_G + \vec{F}_e$$

The primary source of disturbing force is due to mass attraction of the satellite. Other sources are due to the capacitive position sensor and magnetic interactions. The design goal is to build a DFS such that the proof mass is solely under the influence of gravity forces external to the spacecraft, i.e., $\vec{F}_e = 0$.

Mass Attraction on the Proof Mass

In the satellite's rotating reference frame, the specific force on the proof mass caused by satellite mass attraction can be approximated by a truncated Taylor series expansion about the sensor-null point, or

$$f_{ex} = f_{ex_o} + \frac{\partial f_{ex}}{\partial x} x_b + \frac{\partial f_{ex}}{\partial y} y_b \quad (4a)$$

$$f_{ey} = f_{ey_o} + \frac{\partial f_{ey}}{\partial y} y_b + \frac{\partial f_{ey}}{\partial x} x_b \quad (4b)$$

where $f_{ex_o}, f_{ey_o}, \partial f_{ex}/\partial x, \partial f_{ex}/\partial y, \partial f_{ey}/\partial y$, and $\partial f_{ey}/\partial x$ are all evaluated at the sensor null point. Lange[2] used the Euler-Hill equations to show that the in-track trajectory position error $h(t)$ caused by in-track forces $f_{eh}(t)$ is

$$h(s)/f_{eh}(s) = (s^2 - 3\omega_o{}^2)/s^2(s^2 + \omega_o{}^2) \quad (5)$$

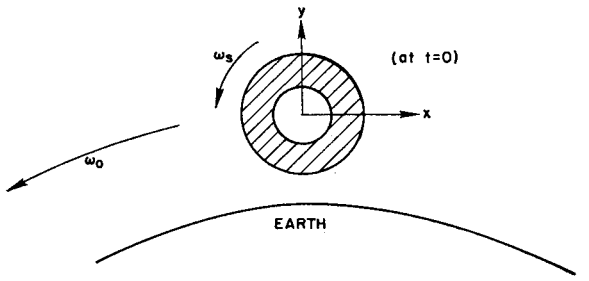

Fig. 1 Initial reference-frame alignment.

where ω_o is defined as the orbital rate ($\simeq 10^{-3}$ rad/sec). If the spin axis of the satellite is normal to the orbit plane and the rotating reference frame is initially ($t = 0$) aligned as in Fig. 1, the specific force in the horizontal and vertical directions (in the orbit plane) is

$$\begin{bmatrix} f_{eh} \\ f_{ev} \end{bmatrix} \triangleq W \begin{bmatrix} f_{ex} \\ f_{ey} \end{bmatrix} \quad (6)$$

Therefore, the horizontal component of mass-attraction specific force is

$$f_{eh} = \left(f_{ex_o} + \frac{\partial f_{ex}}{\partial x} x_b + \frac{\partial f_{ex}}{\partial y} y_b\right)c - \left(f_{ey_o} + \frac{\partial f_{ey}}{\partial x} x_b + \frac{\partial f_{ey}}{\partial y} y_b\right)s \quad (7)$$

The amplitude of the in-track trajectory error caused by sinusoidal f_{eh} is given by the Bode plot of Eq. (5) in Fig. 2 for all frequencies except orbital rate ω_o. This frequency corresponds to the inertially fixed disturbing forces that (for nominally circular orbits) Lange[4] showed yielded secular trajectory errors

$$h(t) = 3 f_{ei}/\omega_o t \quad (8)$$

where f_{ei} is the magnitude of an inertially fixed force acting on the proof mass. For constant f_{eh}, Eq. (5) reduces to

$$h(t) = -\tfrac{3}{2} f_{eh} t^2 \quad (9)$$

The spin rate ω_h will be chosen so that $\omega_h \gg \omega_o$ and, therefore, the mass attraction at the sensor null (f_{ex_o} and f_{ey_o}) contributes negligible trajectory error. (Figure 2 implies that for $|f_{eh}| = f_{ex_o} \simeq 10^{-10}\,g$ and $\omega_h = 0.1$ rad/sec, then $|h(t)| = 10^{-7}$ m.) The need for precise control of the magnitude of of f_{ex_o} and f_{ey_o} is thus eliminated from the design of the satellite by spinning the vehicle.

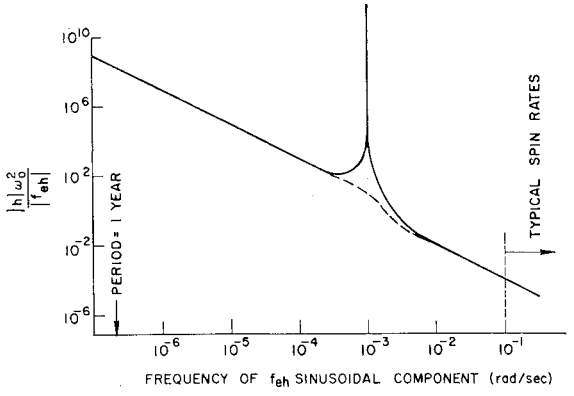

Fig. 2 Amplitude of in-track trajectory errors $h(t)$ due to sinusoidal in-track forces $f_{eh}(t)$.

The effect of the mass-attraction gradient ($\partial f_{ex}/\partial x$, etc.) depends on the time history of x_b and y_b. For the case of a constant horizontal force [see Eq. (3)],

$$\left.\begin{aligned} x_b &= \rho c \\ y_b &= -\rho \mathcal{S} \end{aligned}\right\} \text{ a constant offset in orbit coordinates} \tag{10}$$

where ρ is a constant. Then

$$f_{eh} = (\partial f_{ex}/\partial x + \partial f_{ey}/\partial y)\rho/2 + \text{harmonic terms at } \omega_h \text{ and } 2\omega_h$$

and

$$h(t) = -\frac{3}{2}\left[\frac{(\partial f_{ex}/\partial x) + (\partial f_{ey}/\partial y)}{2}\right]\rho t^2 \tag{11}$$

A spinning drag-free satellite would be designed ideally so that the mass-attraction gradient is zero. It is expected, however, that in actual practice satellites will have a gradient on the order of 10^{-10} g/mm which is a result of the inability to control precisely the weight and location of every mass element in the satellite. As a result, for a spinning satellite experiencing enough atmospheric drag to maintain the condition of Eq. (10) approximately, the in-track trajectory error after one year (3×10^7 sec) is

$$h = 1.5 \times 10^5 \text{m} = 150 \text{ km}$$

which is obtained from Eq. (11), where $[\partial f_{ex}/\partial x) + (\partial f_{ey}/\partial y)]/2 = 10^{-10} g$/mm and $\rho = 0.1$ mm. This would be the largest source of drag-free trajectory errors in spinning satellites; therefore, an integral control law is proposed to attenuate this error.

Integral Controller Equations

The Bode plot in Fig. 2 shows that potentially significant in-track trajectory errors only arise when frequency components of f_{eh} exist at orbital rate or at rates less than 10^{-5} rad/sec (periods greater than approximately 10 days). Typically, the secular errors caused by f_{eh} frequency components at orbital rate (inertially fixed components) are small§; therefore, if the long-term ($\sim$daily) average of f_{eh} is zero, no significant ($\gg 1$ m) in-track trajectory errors can exist. Limiting the integral

$$I_h = \int_o^t f_{eh} dt \tag{12}$$

ensures that the average value of f_{eh} approaches zero and, therefore, this is the criterion for the integral controller. It is convenient also to limit the vertical integral

$$I_v = \int_o^t f_{ev} dt$$

Assuming the mass-attraction model is given by Eq. (4),

$$\begin{aligned} f_{eh} &= c f_{ex_o} - \mathcal{S} f_{ey_o} + C x_{bi} + \Delta C(c_2 x_{bi} + \mathcal{S}_2 y_{bi}) \\ &\quad + C_r(c_2 y_{bi} - \mathcal{S}_2 x_{bi}) \\ f_{ev} &= \mathcal{S} f_{ex_o} + c f_{ey_0} + C y_{bi} + \Delta C(\mathcal{S}_2 x_{bi} - c_2 y_{bi}) \\ &\quad + C_r(c_2 x_{bi} + \mathcal{S}_2 y_{bi}) \end{aligned} \tag{13}$$

Because f_{ex} and f_{ey} are derivable from a potential function, $\partial f_{ex}/\partial y$ must equal $\partial f_{ey}/\partial x$ and, therefore, terms depending on the difference between these two quantities do not appear in Eqs. (13). Depending on ΔC and C_r, the terms in Eqs. (13) will have an effect on the average value of f_{eh} and f_{ev} and long-term effect on I_h and I_v only if $x_{bi}(t)$ and $y_{bi}(t)$ contain a frequency component at $2\omega_h$ or have a nonzero average value. The effect of containing a frequency component at $2\omega_h$ is considered in the error analysis. As a result,

$$\begin{bmatrix} I_h \\ I_v \end{bmatrix} \cong C \int_o^t \begin{bmatrix} x_{bi} \\ y_{bi} \end{bmatrix} dt \tag{14}$$

and the desired integral controller can be mechanized without requiring knowledge of the mass-attraction force gradient by limiting the following integrals:

$$\begin{bmatrix} I_{hc} \\ I_{vc} \end{bmatrix} = \int_o^t \begin{bmatrix} x_{bi} \\ y_{bi} \end{bmatrix} dt = \int_o^t W \begin{bmatrix} x_b \\ y_b \end{bmatrix} dt \tag{15}$$

This is accomplished by introducing a control center bias,

$$\begin{bmatrix} x_u \\ y_u \end{bmatrix} = -k_c W^{-1} \begin{bmatrix} I_{hc} \\ I_{vc} \end{bmatrix} \tag{16}$$

in the control law,

$$f_{cx} = k_p[x_b + x_u + \gamma(\dot{x}_b - \omega_s y_b)] \tag{17a}$$

$$f_{cy} = k_p[y_b + y_u + \gamma(\dot{y}_b + \omega_s x_b)] \tag{17b}$$

The equations of motion of the controlled system, Eqs. (1) and (17), show that for a constant disturbance, the horizontal integral is limited and reaches a steady-state value

$$[I_h]_{ss} = [C|f_i|/k_c k_p] \tag{18}$$

and, after one year, $h = 0.5$ m if

$$|f_i|/k_p = 0.1 \text{ mm}, \; C = 10^{-10} \, g/\text{mm}, \; k_c = 2 \times 10^{-2} \text{ sec}^{-1}$$

This is an error similar to initial injection uncertainties that also propagate linearly with time.[4] Once established, however, the orbit is drag free, and secular trajectory errors exist only with respect to other drag-free orbits with different initial conditions.

Stability

Generally, one would choose values for k_c as high as possible to minimize trajectory errors that arise during the transient behavior of the controller [as in Eq. (18)]. However, an upper limit on k_c is dictated by stability considerations.

Using the frequency symmetry technique,[2,5] the homogeneous controlled equations

$$\ddot{x}_b - (\omega_s^2 - k_p)x_b - \gamma\omega_s k_p y_b + \gamma k_p \dot{x}_b - 2\omega_s \dot{y}_b + k_p x_u = 0 \tag{19a}$$

$$\ddot{y}_b - (\omega_s^2 - k_p)y_b + \gamma\omega_s k_p x_b + \gamma k_p \dot{y}_b + 2\omega_s \dot{x}_b + k_p y_u = 0 \tag{19b}$$

can be reduced to a single complex equation¶

$$\begin{aligned} &\ddot{\eta} + (2j\omega_s + k_p\gamma)\dot{\eta} - (\omega_s^2 - k_p - j\omega_s k_p\gamma)\eta \\ &\quad + k_p k_c\left\{e^{-j\omega_s t}\int_o^t e^{j\omega_s t}\,\eta dt\right\} = 0 \end{aligned} \tag{20}$$

yielding a characteristic equation:

$$s^2 + (2j\omega_s + k_p\gamma)s - (\omega_s^2 - k_p - j\omega_s k_p\gamma) + k_p k_c/(s + j\omega_s) = 0 \tag{21}$$

A locus vs k_c of the complex equation is drawn in Fig. 3 for typical values of the control parameters where the poles consist of the roots of the system without integral control and $s = +j\omega_s$. The figure shows that instability results for values of k_c greater than some critical value. The transformation[2]

$$s' = s + j\omega_s$$

§ Assuming a proof-mass offset = 0.1 mm in a nonrotating reference frame, a mass-attraction gradient = 10^{-10} g/mm (yielding $f_{ei} = 10^{-11} g$ or 10^{-10} m/sec^2), and an orbital rate $\omega_o = 10^{-3}$ rad/sec, Eq. (8) indicates that $h = 9$ m/yr.

¶ Assumes $\omega_s = \omega_h$, a valid approximation since $\omega_s = \omega_h + \omega_o$ and ω_h will typically be 0.1 rad/sec or greater and ω_o is typically 10^{-3} rad/sec.

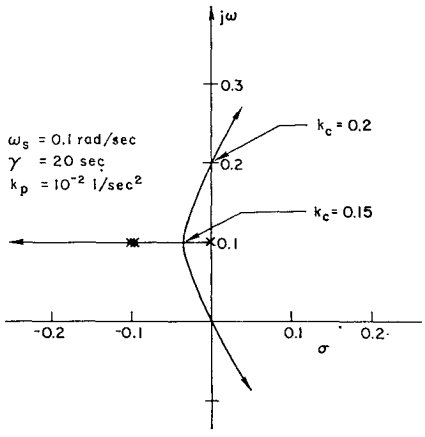

Fig. 3 Root locus plot vs k_c.

shifts the characteristic equation into a nonrotating reference frame, yielding

$$s'^3 + \gamma k_p s'^2 + k_p s' + k_p k_c = 0 \tag{22}$$

Using Routh's criterion, the upper limit on k_c is simply

$$k_c < \gamma k_p \tag{23}$$

a result which also holds for the spinning reference frame because the locus undergoes only a vertical shift on the s plane during retransformation.

Controller with Deadspace

It is anticipated that in the actual implementation of any DFS control system, on-off gas jets will be used to provide the control force. In this case, a deadspace is included to eliminate chatter about the null point and to reduce the influence of noise. In such a control implementation, the previous linear analysis does not strictly apply; therefore, an analog simulation of an integral controller with a square deadspace was made. The deadspace is implemented by adding the function shown in Fig. 4 to each control axis where f_{cx}' and f_{cy}' is the applied control force and f_{cx} and f_{cy} is given by Eqs. (17).

Parameters selected for the simulation are representative of current DFS designs

$$k_c = 0.005, \quad \omega_s = 0.1 \text{ rad/sec}, \quad \gamma = 20 \text{ sec}, \quad k_p = 0.1 \text{ sec}^{-2},$$
$$r_d = 0.1 \text{ mm}$$

Figures 5 and 6 show the responses of the controller simulation during a satellite disturbing force which is constant in a nonrotating reference frame. The position of the proof mass (Fig. 5) in body coordinates oscillates at the spin frequency initially with an amplitude at the deadspace threshold; then the envelope slowly decays at the integral controller time constant. The position of the proof mass in a nonrotating reference frame (Fig. 6) also approaches the deadspace threshold, then slowly returns to the origin. Because the in-track disturbing force on the proof mass, f_{eh}, is proportional to x_{bi} [Eq. (13)], the fact that x_{bi} approaches zero ensures that f_{eh} also approaches zero. This behavior is consistent with that predicted by the linear analysis. For a more complete analog simulation discussion, see Ref. 6.

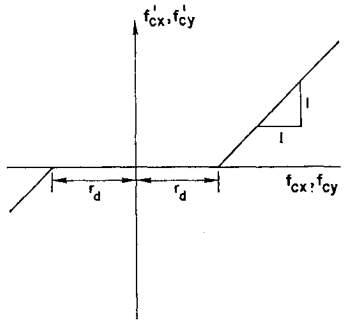

Fig. 4 Square deadspace.

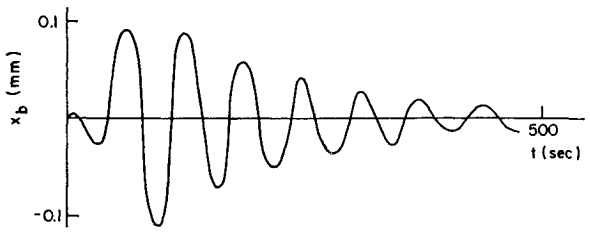

Fig. 5 x_b response with integral controller.

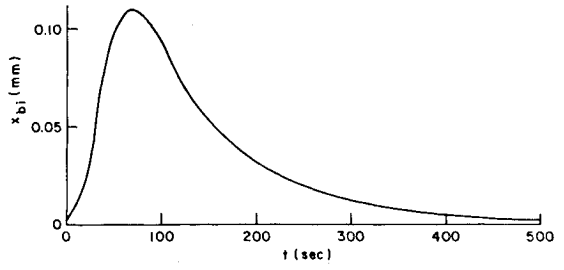

Fig. 6 x_{bi} response with integral controller.

Mechanization Errors

Of primary importance in evaluating the feasibility of an integral controller scheme is how well a mechanization of the controller limits in-track trajectory errors. Because typical trajectory errors generated during transient integral-controller behavior are small [Eq. (18) indicates 1 m], only error sources causing long-term nonzero average values of $f_{eh}(\triangleq \tilde{f}_{eh})$ need be considered, where

$$\tilde{f}_{eh} = \frac{1}{T}\int_0^T f_{eh} dt; \qquad T \simeq 1 \text{ day}$$

Constant atmospheric drag has been shown to be a dominant cause of trajectory errors in a nonintegral controller; therefore, the existence of this condition is assumed while evaluating the trajectory errors of the integral controller. In this condition, an ideal integral controller will cause the in-track force integral to reach a steady-state value, which implies that $\tilde{f}_{eh} = 0$.

Table 1 summarizes the important error sources and their effect. A more comprehensive discussion of the errors is contained in Ref. 1. The magnitudes selected in the table represent reasonable requirements on the integral controller mechanization. For example, the spin rate must be mechanized to within one per cent, and the analog integrator bias is achievable with available operational amplifiers. The attitude control accuracy assumed in the table represents a precision system and is probably the most important error source in the list. The RSS of position errors in the table show an expected combined error of 500 m/yr.

The uncompensated satellite mass-attraction properties utilized in the error predictions require an extensive effort to achieve in drag-free satellite design and fabrication. Although it may be possible (with greater effort and cost) to realize 10^{-10} g normal to the orbit plane and 3×10^{-11} g/mm in plane, it would be much less costly to base the design and

Table 1 Integral controller errors

Error source	Definitions	Relation	Key magnitudes	$\tilde{f}_{eh}$, g	In track trajectory error after 1 yr, m
Spin rate $\bar{\omega}_h - \omega_h$	$\bar{\omega}_h$ = mechanized spin rate ω_h = actual spin rate	$\tilde{f}_{eh} = \frac{C\rho}{2}\left(\frac{\omega_h - \bar{\omega}_h}{k_c}\right)^2$	$C = 10^{-10}$ g/mm $\rho = 0.1$ mm $k_c = 0.02$ sec^{-1} $\omega_h - \bar{\omega}_h = 10^{-3}$ rad/sec	10^{-14}	150
Yaw attitude error	ψ = angle between spin axis and orbit normal f_{ez_o} = mass attraction along spin axis	$\tilde{f}_{eh} = f_{ez_o}\psi$	$f_{ez_o} = 3 \times 10^{-10}$ g $\psi = 10$ arcsec	1.5×10^{-14}	225
Analog integrator bias	b_c = integrator bias s_c = scale factor	$\tilde{f}_{eh} = C\frac{b_c}{k_c}s_c$	$C = 10^{-10}$ g/mm $b_c = 50$ μV/sec $k_c = 0.02$ sec^{-1} $s_c = 0.1$ mm/V	2.5×10^{-14}	400
Digital integration numerical error	s_c = scale factor i = number of decimal digits	$\tilde{f}_{eh} = \frac{1}{2}C(10^{-i})s_c$	$i = 4$ decimal digits $C = 10^{-10}$ g/mm $s_c = 1$ mm/full scale	5×10^{-15}	75

fabrication on 10^{-9} g normal to the orbit plane and 3×10^{-11} g/mm in plane.

Other values assumed in the error analysis could also be improved (again with greater effort and cost) along with mass-attraction improvement. For example, if 1) the spin-rate error is 3×10^{-4} rad/sec; 2) the attitude error is 1 arcsec; 3) a five decimal digit mechanization is employed; then in-track trajectory errors after one year are approximately 10 m.

Conclusions

Trajectory errors of spinning drag-free satellites are not as sensitive to mass-attraction forces as nonspinning satellites. A typical in-track trajectory error for a spinning satellite without integral control after one year, however, is approximately 150 km, which is significant.

An integral controller has been proposed to attenuate this error. The effect of mechanization errors of this controller is that the in-track trajectory error can be reduced to 500 m/yr. This assumes an analog mechanization of the controller equations, a satellite spin-axis misalignment with the orbit plane normal of no more than 10 arcsec and a spin rate ω_h mechanization error of 0.001 rad/sec, where $\omega_h = 0.1$ rad/sec. No knowledge of the mass-attraction properties of the satellite is required; however, the error predictions are based on the mass-attraction gradient in the orbit plane being less than 10^{-10} g/mm and the mass-attraction force normal to the orbit plane being less than 3×10^{-10} g.

References

[1] Powell, J. D. and Lange, B. O., "Control of a Spinning Drag-Free Satellite with an Application of Estimation Theory," SUDAAR Rept. 402, May 1970, Stanford Univ., Stanford, Calif.

[2] Lange, B. O., "Control and Use of Drag-Free Satellites," SUDAAR Rept. 194, June 1964, Stanford Univ., Stanford, Calif.

[3] Sorensen, J. A., "A Magnetic Attitude Control System for an Axisymmetric Spinning Spacecraft," *Journal of Spacecraft and Rockets*, Vol. 8, No. 5, May 1971, pp. 441–448.

[4] Lange, B. O., "The Drag-Free Satellite," *AIAA Journal*, Vol. 2, No. 9, Sept. 1964, pp. 159–1606.

[5] Lange, B. O., Fleming, A. W., and Parkinson, B. W., "Control Synthesis for Spinning Aerospace Vehicles," *Journal of Spacecraft and Rockets*, Vol. 4, No. 2, Feb. 1967, pp. 142–150.

[6] Jhin, P., "Control of a Spinning Drag-Free Satellite to Reduce Trajectory Errors due to Mass Attraction," SUDAAR Rept. 408, Aug. 1970, Stanford Univ., Stanford, Calif.